The transcription factor *Fezf2* directs the differentiation of neural stem cells in the subventricular zone toward a cortical phenotype

Annalisa Zuccotti[1], Corentin Le Magueresse[1,2], Min Chen, Angela Neitz, and Hannah Monyer[3]

Department of Clinical Neurobiology, University Hospital and German Cancer Research Center Heidelberg (DKFZ), 69120 Heidelberg, Germany

Postnatal neurogenesis in mammals is confined to restricted brain regions, including the subventricular zone (SVZ). In rodents, the SVZ is a lifelong source of new neurons fated to migrate to the olfactory bulb (OB), where the majority become GABAergic interneurons. The plastic capacity of neonatal and adult SVZ stem/progenitor cells is still largely unknown. By overexpressing the transcription factor Fezf2, a powerful master gene specifying the phenotype of glutamatergic subcerebral projecting neurons, we investigated whether the fate of postnatally generated SVZ neurons can be altered. Following lentiviral delivery of Fezf2 in the neonatal and adult SVZ niche, we showed that ectopic Fezf2 expression is sufficient to redirect the fate of SVZ stem cells. Thus, based on in vivo and in vitro experiments, we provide evidence that numerous Fezf2-positive OB neurons expressed glutamatergic pyramidal cell molecular markers instead of developing a GABAergic identity. Overexpression of Fezf2 had no effect on transit-amplifying progenitors or neuroblasts but was restricted to neural stem cells. Fezf2-respecified neurons bore features of pyramidal cells, exhibiting a larger cell body and a more elaborate dendritic tree, compared with OB granule cells. Patch-clamp recordings further indicated that Fezf2-respecified neurons had synaptic properties and a firing pattern reminiscent of a pyramidal cell-like phenotype. Together, the results demonstrate that neonatal and adult SVZ stem cells retain neuronal fate plasticity.

respecification | adult stem cell plasticity

Neurogenesis, migration and subsequent integration of newborn neurons into preexisting networks persist in the postnatal brain. In rodents, two neurogenic zones generate neurons in the early postnatal period: the subgranular zone (SGZ) of the hippocampal dentate gyrus (DG) and the subventricular zone (SVZ) of the lateral ventricles (1). Neurogenesis continues throughout postnatal development and into adulthood, albeit at a lower level (2). The SVZ comprises different cell types. Astrocyte-like stem cells give rise to transit-amplifying cells (fast proliferating progenitors) that, in turn, develop into immature neurons (neuroblasts) (3). Newly generated neuroblasts migrate in chains in a well-delineated pathway, the rostral migratory stream (RMS), to their final destination in the olfactory bulb (OB), where they differentiate into distinct neuronal subtypes. The largest fraction of newborn cells, the granule cells, develops a GABAergic phenotype, and they eventually populate the granular cell layer (3). Granule cells are unique with respect to their morphology as well as their connectivity within the local network. Thus, unlike most neurons in the brain, they are axonless and communicate with their neuronal partners (i.e., mitral cells, tufted cells) via reciprocal dendrodendritic synapses (4). Granule cells are hence distinct from other SVZ-derived postnatally generated neurons that also populate the OB. These include glutamatergic neurons (5) and inhibitory and dopaminergic periglomerular cells (6). Given this neuronal diversity, one wonders whether and to what extent neural stem/progenitor cells retain plastic capacities during postnatal development and beyond.

Previous work has shown that retroviral-mediated expression of Ascl1 (Mash1) in the SGZ of DG progenitors is sufficient to instruct newborn cells to differentiate into oligodendrocytes instead

of granule cells (7). Similarly, Olig2 overexpression in the SVZ is enough to suppress neuronal differentiation in favor of oligodendrogliogenesis (8). Moreover, the proportion of dopaminergic periglomerular cells in the population of newborn neurons increased following overexpression of Pax6, a transcription factor involved in the specification of dopaminergic OB neurons (9). Nevertheless, evidence that the progeny of postnatal neural stem/progenitor cells can be redirected toward other neuronal cell types has remained scarce. When successful, the manipulations were performed during either embryonic or early postnatal development. For instance, ectopic expression of the transcription factor Fezf2, essential in the differentiation of layer 5b subcortical projection neurons (10), redirected striatal progenitors, which normally give rise to GABAergic medium spiny neurons, to develop into glutamatergic projection neurons (11). Similarly, callosal projection neurons in layer 2/3 and spiny neurons in layer 4, could be reprogrammed at neonatal stages into layer 5b neurons (12, 13). These studies identified Fezf2 as a master gene for glutamatergic layer 5b neurons.

Here, we sought to determine whether the fate of SVZ stem cells/progenitor cells could be redirected toward a cortical phenotype using ectopic Fezf2 expression. We used lentiviruses and retroviruses to express Fezf2 in the SVZ in vivo. Fezf2 redirected the differentiation of SVZ stem cells. Thus, stem cells that would have normally become OB GABAergic granule cells developed a glutamatergic phenotype.

Results

Fezf2 Alters the Molecular and Morphological Identity of SVZ-Generated Neurons. To determine whether postnatally generated neurons can undergo direct lineage respecification, we injected a mix of two

---

Significance

To study whether and to what extent neuronal stem cells can be reprogrammed postnatally and in the adult is of great importance because they hold the potential to treat neurological diseases for which there are no remedies so far. In the postnatal brain, neurogenesis is restricted to two brain regions: The subventricular zone (SVZ) gives rise to new neurons that preferentially develop a GABAergic phenotype, whereas in the dentate gyrus, glutamatergic neurons are produced. In this study, we took recourse to virus-mediated gene expression, and by introducing a key gene that is normally expressed in glutamatergic pyramidal neurons into SVZ-derived stem cells, we changed their GABAergic fate.
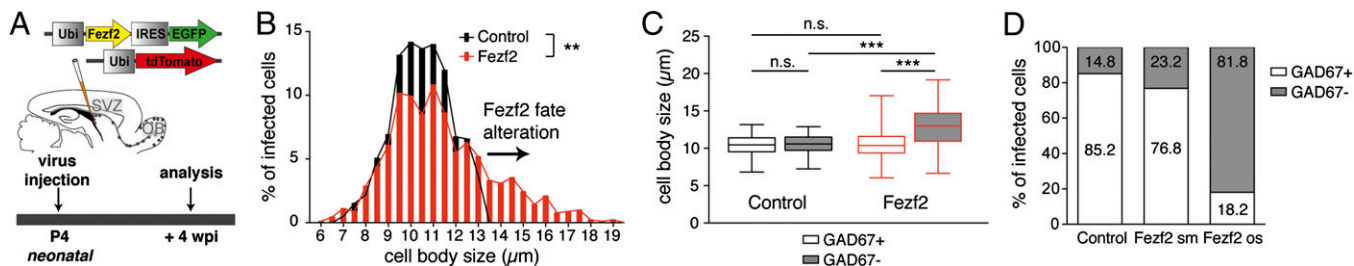
Fig. 1. Fezf2-expressing cells have a larger cell body and are not GABAergic. (*A*) Lentiviruses expressing tdTomato and Fezf2-EGFP were mixed and injected into the SVZ of P4 mice and analyzed 4 wpi (*n* = 10 mice). (*B*) Frequency distribution of the cell body size of control and Fezf2 cells [bin width = 0.5 μm; **P = 0.0018, Kolmogorov–Smirnov (K-S) test]. (*C*) Whiskers graph for control and Fezf2 neurons subdivided into GAD67$^+$ and GAD67$^-$ (one-way ANOVA; ***P < 0.001, Bonferroni multiple comparison post hoc test). n.s., not significant. (*D*) Stacked bar graph showing that most oversized (os) Fezf2$^+$ cells lost their GABAergic phenotype (P < 0.0001, Fisher's exact test).

lentiviruses into the SVZ of 4-d-old mice, (i.e., around the peak time of postnatal OB granule cell genesis) (14). One controlled the coexpression of Fezf2 and EGFP, and the second, serving as a control, directed TdTomato expression (Fig. 1*A*). Four weeks postinjection (wpi), the proportion of control and Fezf2$^+$ cells reaching the OB was similar, indicating that Fezf2 overexpression did not alter cell proliferation and survival (Fig. S1*A*). The layer distribution of Fezf2$^+$ and control cells within the OB was comparable, meaning that the final destination of newborn cells was not changed following ectopic Fezf2 expression (Fig. S1*B*). However, Fezf2$^+$ cells possessed a larger cell body than control cells (Fig. 1*B*). The diameter of a cell body never exceeded 13 μm in control cells, whereas 21.3% of Fezf2$^+$ neurons had a diameter larger than 13 μm (Fig. 1*B*). Similar results were obtained at later time points (Fig. S1*C*). To investigate whether Fezf2 expression altered the cellular phenotype, we first investigated the expression of glutamic acid decarboxylase 67 (GAD67), an enzyme necessary for GABA synthesis and a molecular marker of GABAergic interneurons, in control and Fezf2$^+$ cells. Quantification of GAD67 expression in control and Fezf2$^+$ cells revealed that 85% of control granule cells were immunopositive for GAD67 (GAD67$^+$). As expected, cell body size was similar in GAD67$^-$ and GAD67$^+$

control cells at 4 wpi (Fig. 1*C*). In contrast, only 65% of Fezf2$^+$ cells expressed GAD67, and GAD67$^-$/Fezf2$^+$ cells had a significantly larger cell body than GAD67$^+$/Fezf2$^+$ cells (Fig. 1*C*), suggesting that large Fezf2$^+$ cells were mainly those lacking GAD expression. To test this hypothesis, we divided Fezf2$^+$ cells into "small" (cell body diameter ≤13 μm) and "oversized" (cell body diameter >13 μm) cells. A total of 76.8% of small Fezf2$^+$ cells also expressed GAD67, similar to control cells, whereas only 18.2% of oversized Fezf2$^+$ cells were GAD$^+$ (Fig. 1*D*). These results indicate that small Fezf2$^+$ cells remained GABAergic, similar to control cells, whereas most oversized Fezf2$^+$ cells were respecified. To determine whether SVZ-derived neurons can also undergo lineage respecification in adult stages, we injected the viral mix into the SVZ of adult mice. Four wpi, Fezf2$^+$ cells possessed a larger cell body than control cells (Fig. 2 *A*–*C*). Similar to neonatal stages, Fezf2 expression altered the cellular phenotype. Only 70% of Fezf2$^+$ cells expressed GAD67 (Fig. 2*A*), and GAD67$^-$/Fezf2$^+$ cells had a significantly larger cell body than GAD67$^+$/Fezf2$^+$cells (Fig. 2*D*). Specifically, 86.8% of small Fezf2$^+$ cells expressed GAD67, similar to control cells, whereas only 4.5% of oversized Fezf2$^+$ cells were GAD$^+$ (Fig. 2*E*).

Together, these results show that Fezf2 can redirect the differentiation of SVZ-derived neurons at neonatal and adult
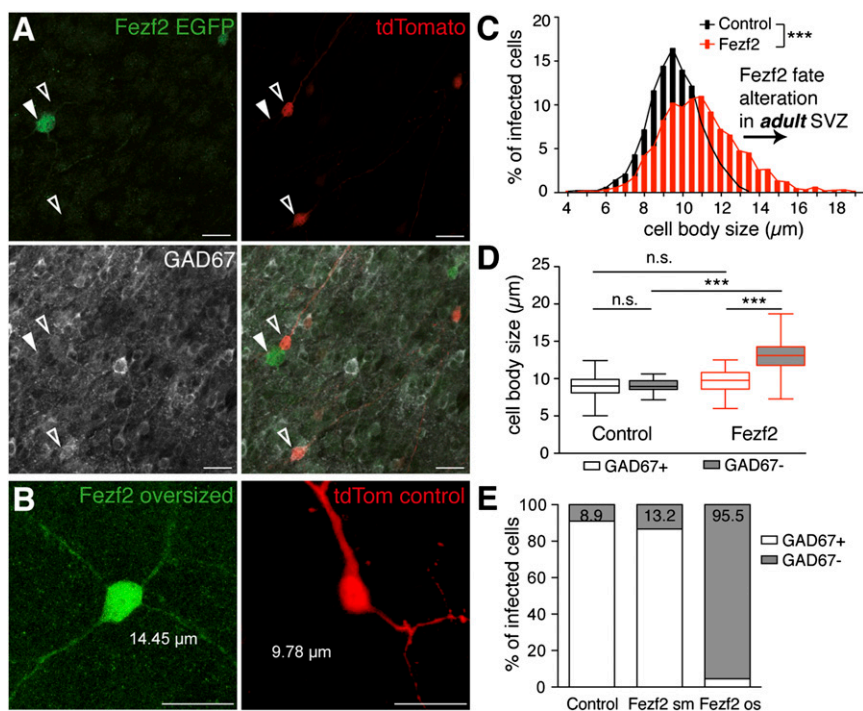

Fig. 2. Altered phenotype of Fezf2-expressing cells in adults. (*A*) Immunohistochemistry for Fezf2-EGFP, tdTomato, and GAD67 analyzed 4 wpi of the viral mix in adult SVZ (*n* = 10 mice). Open arrowheads indicate control tdTomato$^+$/GAD67$^+$ cells. The filled arrowhead indicates a typical oversized Fezf2$^+$/GAD67$^-$ cell. (Scale bars: 20 μm.) (*B*) High magnification of a Fezf2 oversized neuron with a larger body size (14.45 μm) than control granule cells (9.78 μm). (Scale bars: 20 μm.) (*C*) Frequency distribution of cell body size of control and Fezf2 cells (bin width = 0.5 μm; ***P < 0.001, K-S test). (*D*) Whiskers graph for control and Fezf2 neurons subdivided in GAD67$^+$ and GAD67$^-$ (one-way ANOVA; ***P < 0.001, Bonferroni multiple comparison post hoc test). (*E*) Stacked bar graph showing that most oversized (os) Fezf2$^+$ cells lost their GABAergic phenotype (P < 0.0001, Fisher's exact test).

stages. Fezf2-mediated changes of the neuronal phenotype involve the development of a larger cell body and the acquisition of a non-GABAergic fate. Because Fezf2-mediated lineage respecification was quantitatively similar in neonates and in adult mice, we performed subsequent experiments in mice aged postnatal day 2 (P2)–P4 to take advantage of the high level of OB neurogenesis in neonates.

To study the morphological features of neurites in Fezf2-respecified cells, we injected the lentivirus mix into the SVZ of P4 mice (Fig. 1A); 3 to 6 wk later, we used OB slices and performed biocytin filling and morphological reconstruction of whole-cell patch-clamped Fezf2$^+$ and control neurons. The two cell populations could be easily distinguished before patching, based on cell body diameter (>13 µm vs. <13 µm, respectively; Fig. 1B). Control and small Fezf2$^+$ cells showed the typical morphology of OB granule cells, namely, a small cell body, a radial peripheral process extending to the external layers, where it ramifies, and the absence of an axon (Fig. 3 A and B). In contrast, oversized Fezf2$^+$ cells had elaborate dendritic processes with no preferred orientation along the radial axis (Fig. 3C). Dendritic length analysis and Sholl analysis confirmed that length and complexity were increased only in oversized Fezf2$^+$ neurons (Fig. 3 D and E).

Although Fezf2 expression altered the dendritic morphology, it did not suffice to instruct axonal growth. Thus, all processes emanating from oversized Fezf2$^+$ cells were dendrites harboring dendritic spines. Spine density was slightly but significantly decreased in oversized Fezf2$^+$ neurons (Fig. 3F), although the total number of spines per neuron was not lower than in control cells

due to the presence of longer dendrites. Interestingly, spine density was significantly increased in small Fezf2$^+$ cells (Fig. 3F).

The Ability of Fezf2 to Induce a Glutamatergic Neuronal Fate Is Confined to Stem Cells. To assess whether SVZ-derived respecified Fezf2$^+$ cells are glutamatergic, we studied the expression of VGlut1, a glutamate transporter expressed by cortical pyramidal neurons, in neonatally injected mice. Stainings in the granule cell layer (GCL) of the OB prevented the unambiguous detection of VGlut1 in Fezf2$^+$ cells, because numerous axon terminals in the GCL expressed VGlut1 and rendered colocalization attempts difficult. Therefore, we analyzed VGlut1 mRNA expression by single-cell RT-PCR after harvesting in the patch pipette the cell content of Fezf2 oversized or control neurons (Fig. 4A). Most Fezf2 oversized neurons (seven of eight oversized neurons) expressed VGlut1, whereas no control cell (zero of five control cells) was positive for VGlut1. Moreover, to verify VGlut1 expression at the protein level, we took recourse to primary cultures in which neural stem/progenitor cells from the postnatal SVZ were allowed to proliferate and form neurospheres. Shortly before differentiation into neurons, neurospheres were infected with either the virus encoding for Fezf2 and GFP or the virus encoding for tdTomato. Only 14.16 ± 3.003% of control neurons expressed VGlut1 (Fig. 4 B and C), in line with the reported finding that a limited number of glutamatergic neurons derived from the SVZ (5). Significantly more Fezf2$^+$ neurons expressed VGlut1 (Fig. 4 C and D; 88.40 ± 3.136).

To corroborate further the glutamatergic nature of Fezf2$^+$ neurons, we performed patch-clamp recordings in SVZ-derived neurons. In control neurons, brief voltage steps elicited currents that were blocked by gabazine but not by 6-cyano-7-nitroquinoxaline-2,3-dione (CNQX). In contrast, responses in Fezf2$^+$ neurons were blocked by either CNQX or gabazine (Fig. 4E). Because responses obtained in control and Fezf2$^+$ neurons had similar rise times and decay times (Fig. S2) and were very different from AMPA receptor- or kainate receptor-mediated responses, we concluded that they were all GABAergic. The most likely explanation that can account for this observation is as follows: the patch-clamped Fezf2$^+$ cell releases glutamate that excites a postsynaptic GABAergic neuron, which, in turn, phasically releases GABA onto the patch-clamped neuron (Fig. 4F).

We examined the expression of CRYM, TLE4, and Bhlhb5 (i.e., proteins that are specific to corticofugal projection neurons) (15). Three days after differentiation, 90.1 ± 6.6% of Fezf2$^+$ neurons but only 4.09 ± 2.9% of control neurons were positive for CRYM (Fig. S3). However, neither Fezf2$^+$ neurons nor controls were positive for CRYM at 14 d, or for Bhlh5 and TLE4 at 3 or 14 d after differentiation. Moreover, we investigated CRYM expression in the RMS at 5, 7, and 10 d and in the OB at 4 wk after injection into P4 mice. CRYM was never expressed in either Fezf2$^+$ or control neurons, indicating that Fezf2 expression alone does not completely suffice to switch the phenotype of olfactory granule cells to layer V pyramidal neurons.

In summary, the ectopic expression of Fezf2 into the SVZ can instruct newborn neurons to become pyramidal-like glutamatergic neurons instead of GABAergic granule cells. Interestingly in comparison to the ~17–20% respecified neurons observed in vivo, the in vitro experiments revealed a much higher Fezf2 efficacy. Indeed, in cultured neurospheres, Fezf2 targets a pure stem cell-like population (16). Under in vivo conditions, lentiviruses transduce all cells at the injection site, including slowly dividing stem cells (Fig. S4), progenitor cells, and neuroblasts. We therefore hypothesized that ectopic Fezf2 expression may redirect cell fate only when expressed in stem cells, as suggested by the in vitro assay. To follow up on this hypothesis, we specifically targeted progenitor cells using retroviral injections in the SVZ (Fig. S5A), because the nature of the retrovirus guarantees the exclusive infection of dividing cells (17). We injected the virus mix into the SVZ of P4 mice and analyzed them at 4 and 8 wpi. Infected cells expressing Fezf2 were positive for the tdTomato protein, whereas control cells were positive for EGFP (Fig. S5A). Only 1% of
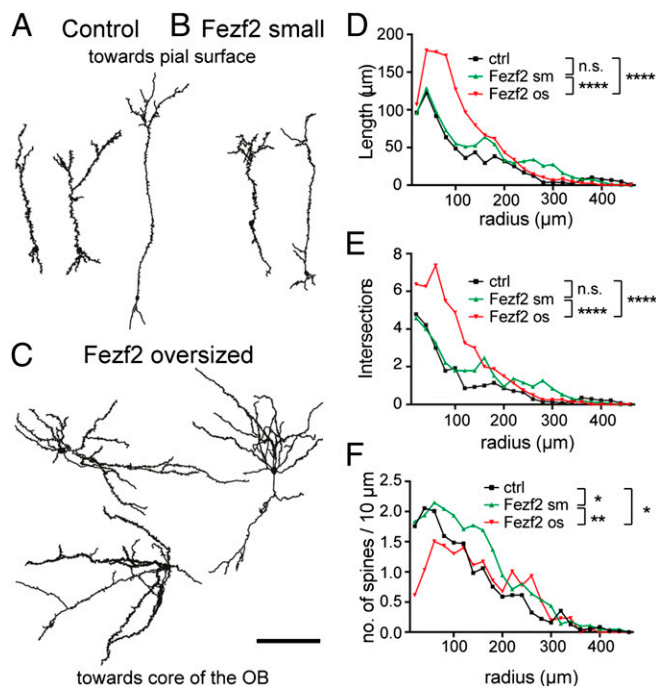

Fig. 3. Oversized Fezf2$^+$ cells display a more elaborate dendritic morphology. Representative camera lucida drawings of biocytin-filled control bulbar granule cells (A), small Fezf2$^+$ cells (B), and respecified Fezf2$^+$ cells (C) more than 3 wpi of the viral mix in P4 mice. (Scale bar: 100 µm.) Sholl analysis of the cell process length shows significant differences in the length of dendrites (D) and intersections of cell processes (E) (two-way ANOVA with a Bonferroni multiple comparison test). (F) Number of dendritic spines normalized to the corresponding cell process length (spine density) (two-way ANOVA with a Bonferroni multiple comparison test). Error bars were omitted for clarity, and data points indicate means (n = 14/6 cells/mice for control (ctrl), n = 19/9 cells/mice for Fezf2 small (sm), and n = 8/8 cells/mice for Fezf2 os). *P < 0.05; **P <0.01; ****P < 0.0001; n.s., not significant.
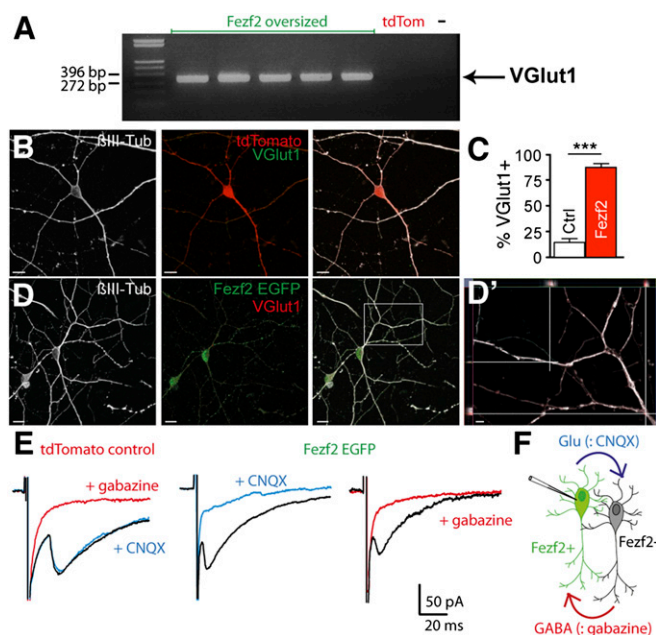
Fig. 4. Fezf2 induces a glutamatergic phenotype. (*A*) Single-cell RT-PCR detection of VGlut1 (expected size = 311 bp) in Fezf2 oversized (*n* = 8/3 cells/mice) but not in TdTomato control (*n* = 5/2 cells/mice) cells. −, negative control (i.e., water). Neurosphere-derived control neurons (tdTomato, red) do not express VGlut1 (*B*; green), whereas Fezf2$^+$ neurons (green) express VGlut1 (*D*; red). (Scale bars: *B* and *D*, 10 μm). βIII Tubulin (βIII-Tub; white) was used as a neuronal marker. (*D'*) Orthogonal projections show VGlut1$^+$ particles (red) in neuronal processes (white). (Scale bar: 2 μm). (*C*) Total of 88.40 ± 3.003% of Fezf2$^+$ neurons and 14.16 ± 3.136% of control neurons are VGlut1$^+$ (*n* = 5 neurosphere preparations, *n* = 98 Fezf2$^+$ cells vs. *n* = 90 control neurons, *t* test, ***P < 0.001). (*E* and *F*) Voltage steps (1 ms) elicited inward currents blocked by gabazine (10 μM) but not CNQX (10 μM) in control neurons 3 wk after differentiation (five of five neurons). In Fezf2$^+$ neurons, inward currents were always blocked by either gabazine (five of five neurons) or CNQX (seven of seven neurons), suggesting that Fezf2$^+$ neurons form glutamatergic synapses with neighboring GABAergic cells, which, in turn, releases GABA onto the patch-clamped neuron as shown in the schematic drawing (*F*).

Fezf2$^+$ cells had a cell body larger than 13 μm (Fig. S5*B*). This percentage is significantly lower than that observed after lentiviral-mediated expression of Fezf2 (~20%; Fig. S5*B*), suggesting that fast-dividing progenitors are insensitive to Fezf2-mediated respecification. Similar results were obtained at 8 wpi (~3.5%, five of 138 cells).

Next, migrating neuroblasts were specifically targeted by injecting the lentiviral mix into the middle part of the RMS of P8 mice (Fig. S5*C*). Four weeks later, the cell body size was analyzed for Fezf2-expressing and control neurons in the OB, and no difference was found between the two groups (Fig. S5*D*). Taken together, these results indicate that ectopic Fezf2 expression in vivo does not reprogram fast-dividing progenitors or postmitotic immature migrating neuroblasts. Together with the results obtained in vitro, we conclude that Fezf2 can only efficiently respecify slow-dividing stem cells in the SVZ.

Considering the small fraction of Fezf2-redirected cells following lentivirus injections in vivo, one wonders whether only a particular subpopulation of neural stem cells is responsive to Fezf2 expression [i.e., those that are predominantly located in the dorsal SVZ and eventually will generate glutamatergic juxtaglomerular neurons (5)]. However, based on two lines of results, we can refute this hypothesis. First, we selectively targeted the dorsal or lateral stem cell niche of the SVZ in neonatal mice using electroporation (18) of Fezf2-GFP and tdTomato plasmids (Fig. S6*A*). Analysis of the OB 4 wk after electroporation

revealed the presence of oversized Fezf2 cells in both conditions (Fig. S6*B*), thus excluding a specific effect of Fezf2 on either subset of stem cells. Accordingly, a similar fraction of Fezf2$^+$ neurons derived from the dorsal or lateral SVZ expressed the glutamatergic marker VGlut1 (Fig. S6*C*). Second, Fezf2$^+$ migrating neurons expressed neither Tbr2 nor Tbr1 (Fig. S6 *D and E*), two transcription factors that are sequentially expressed in the precursor cells of glutamatergic juxtaglomerular neurons (5).

Fezf2 Directs Functional Properties Toward a Cortical Pyramidal Cell Phenotype. To study whether electrophysiological features of Fezf2-respecified cells were different from those of control cells, we performed whole-cell patch-clamp recordings in OB slices 3 to 6 wk after injection of Fezf2. Because electrophysiological recordings of respecified neurons in adult mice were technically extremely difficult, we performed recordings in juvenile mice that were injected at P4 (Fig. 1*A*). Although passive electrophysiological properties were similar in control cells and small Fezf2$^+$ cells, oversized Fezf2 cells showed an increased membrane time constant, decreased membrane resistance, and higher capacitance, consistent with the larger cell body and more elaborate dendritic tree of Fezf2-respecified neurons (Fig. 5 *A–D*). The action potential waveform (Fig. S6*A*) was altered in oversized but not in small Fezf2$^+$ cells. Thus, in oversized Fezf2$^+$ neurons, the membrane voltage threshold for action potential initiation was lower than in control cells, the action potential amplitude was increased, and the amplitude and latency of the fast hyperpolarization were decreased (Fig. S7 *B–F*). These results indicate that the action potential waveform in oversized Fezf2$^+$ cells is respecified toward cortical pyramidal cell features (19, 20). Upon somatic current injection, OB granule cells exhibit a long lag to spiking (21) (Fig. S7*G*), whereas the lag to spiking is shorter in deep layer cortical pyramidal cells. Indeed, the lag to spiking was shorter in oversized Fezf2$^+$ neurons than in small Fezf2$^+$ neurons and control granule cells (Fig. S7*H*). In addition, like the majority of corticospinal pyramidal neurons, all respecified neurons either fired with progressively longer interspike intervals or showed a brief period of spike frequency adaptation followed by relatively constant interspike intervals (19, 20) (Fig. 6 *A–D*).

To examine whether Fezf2 expression also modifies the synaptic input onto OB granule cells, we recorded miniature excitatory postsynaptic currents (mEPSCs) and miniature inhibitory
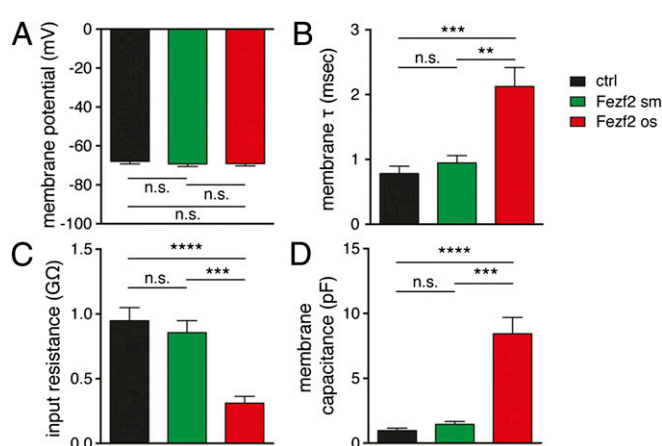

Fig. 5. Passive and active physiological properties are altered in oversized Fezf2$^+$ cells. Electrophysiological recordings of ctrl granule cells (*n* = 20/6 cells/mice), sm Fezf2$^+$ cells (*n* = 19/7 cells/mice), and os Fezf2$^+$ cells (*n* = 15/14 cells/mice) were obtained 20–71 d after injection in P4 mice. Resting membrane potential (*A*) was similar among cell populations, whereas membrane decay τ (*B*), input resistance (*C*), and membrane capacitance (*D*) were significantly different between control and Fezf2 oversized neurons (*A*, one-way ANOVA followed by Tukey's test: *P* = 0.7277; *B–D*, Kruskal–Wallis test followed by Dunn's test: **P < 0.01; ***P < 0.001; ****P < 0.0001).
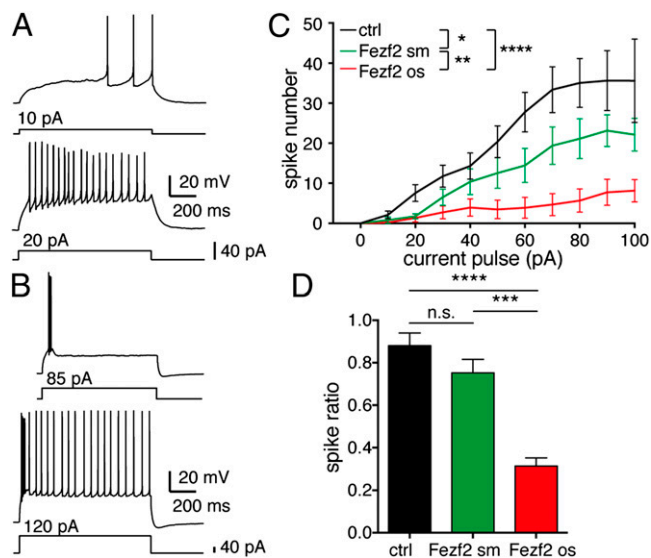
NEUROSCIENCE

Fig. 6. Fezf2-redirected neurons exhibit a pyramidal cell-like firing pattern. Action potential firing patterns of a representative control granule cell (A) and an oversized Fezf2$^+$ cell (B) in response to a depolarizing current injection (Lower). (C) Spike number during 1-s current pulse injections in granule cells (ctrl, n = 20/6 cells/mice), sm Fezf2$^+$ cells (n = 19/7 cells/mice), and os Fezf2$^+$ cells (n = 15/14 cells/mice). Current pulses were injected with increments of 10 pA. Oversized Fezf2$^+$ cells fire action potentials at significantly higher depolarizations than ctrl and sm Fezf2$^+$ cells (two-way ANOVA followed by Bonferroni test: *$P < 0.05$; **$P < 0.01$; ****$P < 0.0001$). (D) Spike ratios show significant different spiking behaviors between the three cell subpopulations (Kruskal–Wallis test followed by Dunn's test: ***$P < 0.001$; ****$P < 0.0001$). Recordings for spike ratios were obtained from the same cells as in B.

postsynaptic currents (mIPSCs) in oversized Fezf2$^+$ and control neurons. The amplitude of mEPSCs was not significantly different in the two groups (Fig. 7 A and B). The frequency of mEPSCs was marginally, although not significantly, increased in oversized Fezf2$^+$ cells (Fig. 7C). However, a cumulative probability histogram revealed that the interevent interval was significantly decreased (Fig. 7D). These results suggest that oversized Fezf2$^+$ cells receive more excitatory synaptic contacts from their neuronal partners, which is in line with the increased dendritic length in respecified neurons. Notably, the decay time constant of mEPSCs was increased by 79% in oversized Fezf2$^+$ cells (Fig. 6E), suggesting that the subunit composition of AMPA receptors at excitatory synapses is altered. These results are consistent with respecification toward cortical pyramidal features, because mEPSC decay time constants in cortical pyramidal cells are, on average, lower than in OB granule cells (22, 23) (Table S1).

The amplitude of mIPSCs was smaller in oversized Fezf2$^+$ cells than in control cells (Fig. 7 F and G). The frequency of mIPSCs was higher in respecified cells, which is indicative of more inhibitory synaptic contacts (Fig. 7 H and I). This may reflect the increased size of soma and dendrites in respecified Fezf2$^+$ neurons. Interestingly, the decay time constant of mIPSCs was markedly decreased in oversized Fezf2$^+$ cells (Fig. 7J), consistent with respecification toward synaptic characteristics of pyramidal cells in cortical layer 5 (23) (Table S1).

Discussion

Here, we demonstrated that the in vivo expression of Fezf2 in SVZ stem cells directs the differentiation of biochemical, morphological, and functional characteristics of SVZ-derived neurons, thus transforming cells destined to become GABAergic granule cells into glutamatergic neurons bearing a number of features characteristic of cortical pyramidal neurons.

Ectopic expression of Fezf2 repressed the GABAergic nature of SVZ-derived neurons in the OB and induced the expression

of the glutamatergic marker VGlut1. Moreover, CRYM, a subcortical projection neuron-specific protein (15) was expressed, at least transiently in vitro, in Fezf2$^+$ SVZ-derived neurons. In addition, electrophysiological properties of oversized respecified Fezf2$^+$ cells resembled those of layer 5 pyramidal cells rather than those of granule cells. Thus, Fezf2 enables the unfolding of a coordinated genetic program that instructs a biochemical, morphological, and functional cellular phenotype reminiscent of corticofugal pyramidal cells. Nevertheless, Fezf2 affected only the fate of stem cells but not that of progenitors or neuroblasts. Some granule cell features were still maintained in respecified neurons, as indicated by the absence of an axon in OB Fezf2$^+$ neurons. Thus, Fezf2 expression generated a "chimeric" neuronal phenotype. Fezf2 expression in SVZ stem cells sufficed to dictate the development of elaborate dendritic processes. In layer 5 subcortical projecting neurons, Fezf2 regulates dendritic morphology and controls axon targeting (24). It is conceivable that the absence of an axon in redirected cells is due to an unfavorable environment (e.g., insufficiency or even absence of a specific trophic support) in the OB. The observed changes,
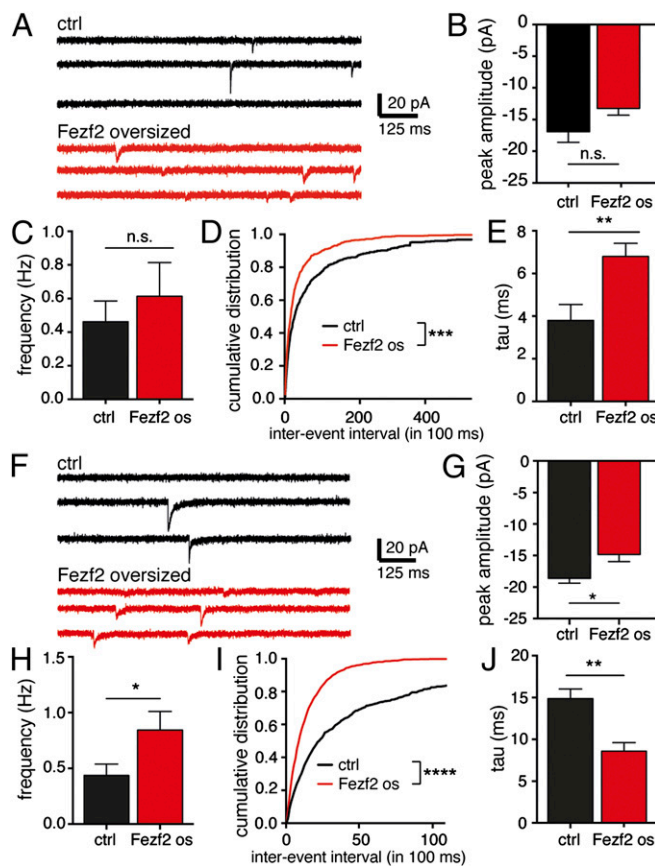

Fig. 7. Synaptic input onto oversized Fezf2$^+$ granule cells is altered. (A) Representative mEPSCs recorded from a control cell (Upper) and a Fezf2$^+$ oversized cell (Lower). mEPSC amplitude (B) and frequency (C) are not significantly changed in Fezf2$^+$ os cells, but a cumulative distribution (D) shows that interevent intervals are significantly shorter in Fezf2$^+$ os cells (***$P < 0.001$, K-S test). (E) Decay time constant of mEPSCs is slower in Fezf2$^+$ os cells (**$P = 0.0051$, t test). (F) mIPSCs recorded from a control cell (Upper) and a Fezf2$^+$ os cell (Lower). Mean mIPSC amplitude is increased (G; *$P = 0.017$) and mIPSC frequency is decreased in Fezf2$^+$ os cells (H; *$P = 0.033$). (I) Cumulative histogram showing that interevent intervals are significantly shorter in Fezf2$^+$ os cells (****$P < 0.0001$, K-S test). (J) Decay time constant of mIPSCs is faster in Fezf2$^+$ os cells (**$P = 0.0033$, t test) (mEPSC ctrl, n = 19/4 cells/mice; mEPSC Fezf2 os, n = 9/7 cells/mice; mIPSC ctrl, n = 16/4 cells/mice; mIPSC Fezf2 os, n = 6/5 cells/mice).

however, occurred despite the ectopic location of the pyramidal-like neurons and were dictated by a single transcription factor. Perhaps the combination of Fezf2 with other fate-modifying factors in a more favorable environment can further enhance the reprogramming efficiency to overcome extrinsic fate specification.

Closely related neuronal types may share a common developmental history, including a similar gene expression profile and a common epigenetic signature (25). Therefore, it was proposed that direct reprogramming may be more efficiently achieved in neuronal subtypes of developmentally related lineages (26). Recent evidence has provided support for this hypothesis. Thus, Fezf2 sufficed to instruct striatal progenitors to switch fate and generate corticofugal-projecting neurons. Interestingly, the Fezf2-induced reprogramming acted at an early postmitotic stage, because molecular markers indicated that striatal progenitors did not adopt an intermediate cortical progenitor identity (11). When Fezf2 was able to reprogram neurons at later stages of neonatal development, the involved neuronal types were more closely related. For instance, Fezf2 expression reprogrammed callosal projection neurons in layer 2/3 and spiny neurons in layer 4 into layer 5b cortical neurons (12, 13). We showed that Fezf2 instructed stem cells of the neonatal and adult SVZ to undergo partial lineage respecification but could not efficiently reprogram progenitor cells or postmitotic neuroblasts. The different capabilities of SVZ transit-amplifying cells and striatal progenitors to be reprogrammed by Fezf2 may reside in their distinct genetic profiles. Thus, in mice, SVZ stem cells/progenitor cells derive mainly from progenitors of the dorsal part of the lateral ganglionic eminence, whereas the origin of striatal neurons can be traced back to progenitors of the ventral lateral ganglionic eminence (27). However, we cannot exclude the possibility that the environment of progenitors in the postnatal SVZ also contributes to restrict the reprogramming potency of progenitor cells.

The molecular mechanism that allows respecification in SVZ stem cells but not in transit-amplifying cells or newborn neurons is unknown. Epigenetic regulation of gene expression may contribute to the decreased reprogramming ability of transit-amplifying cells, because promoter methylation and acquisition of Polycomb repression during the course of neuronal differentiation were shown to restrict pluripotency (28).

Previous studies reported more efficient reprogramming induced by ectopic Fezf2 expression, but the effect was restricted to embryonic development (11) and early stages of postmitotic development in excitatory cortical neurons, terminating around P20 (12, 13). Here, we showed that the effect of Fezf2 in directing the differentiation of SVZ stem cells was not restricted to neonatal development but also occurred in adults. We challenged the potency of adult SVZ stem cells in vivo and showed that their fate is not irrevocably specified.

Materials and Methods

We used WT C57BL/6 mice (Charles River Laboratories), and all procedures were in accordance with the animal care guidelines of the University Hospital and German Cancer Research Center and approved by the local governing committee (Regierungspräsidium Karlsruhe, Germany). Lentivirus and retrovirus with their corresponding control virus were injected into the SVZ or RMS. Neurospheres were infected with lentivirus, and immunostaining of fixed neurons, as well as that of brain tissue, was performed according to standard procedures. Electrophysiological recordings were carried out in sagittal brain slices. For morphological reconstruction, neurons were filled with biocytin, and the Neurolucida software package (MBF Bioscience) was used for analysis. Immunofluorescent images were acquired using a Zeiss confocal microscope (LSM 700) and analyzed with Zen software (Carl Zeiss). Statistical analyses were performed using Prism 5 software (GraphPad) (not significant, $P > 0.05$; *$P < 0.05$; **$P < 0.01$; ***$P < 0.001$; ****$P < 0.0001$). Details are provided in *SI Materials and Methods*.

1. Hatten ME (1999) Central nervous system neuronal migration. *Annu Rev Neurosci* 22: 511–539.
2. Abrous DN, Koehl M, Le Moal M (2005) Adult neurogenesis: From precursors to network and physiology. *Physiol Rev* 85(2):523–569.
3. Lois C, Alvarez-Buylla A (1994) Long-distance neuronal migration in the adult mammalian brain. *Science* 264(5162):1145–1148.
4. Shepherd GM, Chen WR, Willhite D, Migliore M, Greer CA (2007) The olfactory granule cell: From classical enigma to central role in olfactory processing. *Brain Res Brain Res Rev* 55(2):373–382.
5. Brill MS, et al. (2009) Adult generation of glutamatergic olfactory bulb interneurons. *Nat Neurosci* 12(12):1524–1533.
6. Kosaka K, Toida K, Margolis FL, Kosaka T (1997) Chemically defined neuron groups and their subpopulations in the glomerular layer of the rat main olfactory bulb—II. Prominent differences in the intraglomerular dendritic arborization and their relationship to olfactory nerve terminals. *Neuroscience* 76(3):775–786.
7. Jessberger S, Toni N, Clemenson GD, Jr, Ray J, Gage FH (2008) Directed differentiation of hippocampal stem/progenitor cells in the adult brain. *Nat Neurosci* 11(8):888–893.
8. Marshall CA, Novitch BG, Goldman JE (2005) Olig2 directs astrocyte and oligodendrocyte formation in postnatal subventricular zone cells. *J Neurosci* 25(32):7289–7298.
9. Hack MA, et al. (2005) Neuronal fate determinants of adult olfactory bulb neurogenesis. *Nat Neurosci* 8(7):865–872.
10. Molyneaux BJ, Arlotta P, Hirata T, Hibi M, Macklis JD (2005) Fezl is required for the birth and specification of corticospinal motor neurons. *Neuron* 47(6):817–831.
11. Rouaux C, Arlotta P (2010) Fezf2 directs the differentiation of corticofugal neurons from striatal progenitors in vivo. *Nat Neurosci* 13(11):1345–1347.
12. Rouaux C, Arlotta P (2013) Direct lineage reprogramming of post-mitotic callosal neurons into corticofugal neurons in vivo. *Nat Cell Biol* 15(2):214–221.
13. De la Rossa A, et al. (2013) In vivo reprogramming of circuit connectivity in postmitotic neocortical neurons. *Nat Neurosci* 16(2):193–200.
14. Lledo PM, Merkle FT, Alvarez-Buylla A (2008) Origin and function of olfactory bulb interneuron diversity. *Trends Neurosci* 31(8):392–400.
15. Molyneaux BJ, Arlotta P, Menezes JR, Macklis JD (2007) Neuronal subtype specification in the cerebral cortex. *Nat Rev Neurosci* 8(6):427–437.
16. Doetsch F, Petreanu L, Caille I, Garcia-Verdugo JM, Alvarez-Buylla A (2002) EGF converts transit-amplifying neurogenic precursors in the adult brain into multipotent stem cells. *Neuron* 36(6):1021–1034.
17. Ming GL, Song H (2005) Adult neurogenesis in the mammalian central nervous system. *Annu Rev Neurosci* 28:223–250.
18. Fernández ME, Croce S, Boutin C, Cremer H, Raineteau O (2011) Targeted electroporation of defined lateral ventricular walls: A novel and rapid method to study fate specification during postnatal forebrain neurogenesis. *Neural Dev* 6:13.
19. Hattox AM, Nelson SB (2007) Layer V neurons in mouse cortex projecting to different targets have distinct physiological properties. *J Neurophysiol* 98(6):3330–3340.
20. Tseng GF, Prince DA (1993) Heterogeneity of rat corticospinal neurons. *J Comp Neurol* 335(1):92–108.
21. Schoppa NE, Westbrook GL (1999) Regulation of synaptic timing in the olfactory bulb by an A-type potassium current. *Nat Neurosci* 2(12):1106–1113.
22. Schoppa NE (2006) AMPA/kainate receptors drive rapid output and precise synchrony in olfactory bulb granule cells. *J Neurosci* 26(50):12996–13006.
23. Dani VS, et al. (2005) Reduced cortical activity due to a shift in the balance between excitation and inhibition in a mouse model of Rett syndrome. *Proc Natl Acad Sci USA* 102(35):12560–12565.
24. Chen JG, Rasin MR, Kwan KY, Sestan N (2005) Zfp312 is required for subcortical axonal projections and dendritic morphology of deep-layer pyramidal neurons of the cerebral cortex. *Proc Natl Acad Sci USA* 102(49):17792–17797.
25. Bernstein BE, Meissner A, Lander ES (2007) The mammalian epigenome. *Cell* 128(4): 669–681.
26. Rouaux C, Bhai S, Arlotta P (2012) Programming and reprogramming neuronal subtypes in the central nervous system. *Dev Neurobiol* 72(7):1085–1098.
27. Stenman J, Toresson H, Campbell K (2003) Identification of two distinct progenitor populations in the lateral ganglionic eminence: Implications for striatal and olfactory bulb neurogenesis. *J Neurosci* 23(1):167–174.
28. Mohn F, et al. (2008) Lineage-specific polycomb targets and de novo DNA methylation define restriction and potential of neuronal progenitors. *Mol Cell* 30(6): 755–766.

NEUROSCIENCE